Journal for ImmunoTherapy of Cancer

Oral PD-L1 inhibitor GS-4224 selectively engages PD-L1 high cells and elicits pharmacodynamic responses in patients with advanced solid tumors

Jared M Odegard ,[1] Ahmed A Othman ,[2] Kai-Wen Lin,[3] Adele Y Wang,[3] Jonathan Nazareno,[3] Oh Kyu Yoon,[3] John Ling,[3] Latesh Lad,[3] P Rod Dunbar,[4] Dung Thai,[3] Edmond Ang,[5] Nicholas Waldron,[5] Sanjeev Deva[5]

To cite: Odegard JM, Othman AA, Lin K-W, *et al*. Oral PD-L1 inhibitor GS-4224 selectively engages PD-L1 high cells and elicits pharmacodynamic responses in patients with advanced solid tumors. *Journal for ImmunoTherapy of Cancer* 2024;**12**:e008547. doi:10.1136/jitc-2023-008547

► Additional supplemental material is published online only. To view, please visit the journal online (https://doi.org/10.1136/jitc-2023-008547).

Accepted 01 March 2024

[1]Biomarker Sciences, Gilead Sciences Inc, Seattle, Washington, USA
[2]Clinical Pharmacology, Gilead Sciences Inc, Foster City, California, USA
[3]Gilead Sciences, Inc, Foster City, California, USA
[4]School of Biological Sciences and Maurice Wilkins Centre, The University of Auckland, Auckland, New Zealand
[5]University of Auckland, Auckland, New Zealand

Correspondence to
Dr Jared M Odegard; jared.odegard@gmail.com

ABSTRACT

Background Checkpoint inhibitors targeting the programmed cell death 1 (PD-1)/programmed cell death 1 ligand 1 (PD-L1) pathway are effective therapies in a range of immunogenic cancer types. Blocking this pathway with an oral therapy could benefit patients through greater convenience, particularly in combination regimens, and allow flexible management of immune-mediated toxicities.

Methods PD-L1 binding activity was assessed in engineered dimerization and primary cell target occupancy assays. Preclinical antitumor activity was evaluated in ex vivo and in vivo human PD-L1-expressing tumor models. Human safety, tolerability, pharmacokinetics, and biomarker activity were evaluated in an open-label, multicenter, sequential dose-escalation study in patients with advanced solid tumors. Biomarkers evaluated included target occupancy, flow cytometric immunophenotyping, plasma cytokine measurements, and T-cell receptor sequencing.

Results GS-4224 binding caused dimerization of PD-L1, blocking its interaction with PD-1 and leading to reversal of T-cell inhibition and increased tumor killing in vitro and in vivo. The potency of GS-4224 was dependent on the density of cell surface PD-L1, with binding being most potent on PD-L1–high cells. In a phase 1 dose-escalation study in patients with advanced solid tumors, treatment was well tolerated at doses of 400–1,500 mg once daily. Administration of GS-4224 was associated with a dose-dependent increase in plasma GS-4224 exposure and reduction in free PD-L1 on peripheral blood T cells, an increase in Ki67 among the PD-1-positive T-cell subsets, and elevated plasma cytokines and chemokines.

Conclusions GS-4224 is a novel, orally bioavailable small molecule inhibitor of PD-L1. GS-4224 showed evidence of expected on-target biomarker activity, including engagement of PD-L1 and induction of immune-related pharmacodynamic responses consistent with PD-L1 blockade.

Trial registration number NCT04049617.

WHAT IS ALREADY KNOWN ON THIS TOPIC

⇒ An oral checkpoint inhibitor therapy would be promising for patients who could benefit from the increased convenience and unique pharmacology.

WHAT THIS STUDY ADDS

⇒ Orally administered GS-4224 showed preclinical activity similar to anti-programmed cell death 1 ligand 1 (PD-L1) antibodies.

HOW THIS STUDY MIGHT AFFECT RESEARCH, PRACTICE OR POLICY

⇒ In patients with solid tumors, GS-4224 was well tolerated and triggered the pharmacodynamic responses expected from PD-L1 blockade.

INTRODUCTION

The inhibitory receptor programmed cell death 1 (PD-1) is a key negative regulator of T-cell function that acts as a checkpoint on the maintenance of ongoing antitumor T-cell responses. PD-1 has two ligands, programmed cell death 1 ligand 1 (PD-L1) and programmed cell death 1 ligand 2 (PD-L2), with the former playing a key role in limiting tumor immunity.[1] Immune checkpoint inhibitors (ICIs), including therapeutic antibodies that block either PD-1 or PD-L1, have emerged as effective treatment options in a range of immunogenic cancer types. Eight antibodies targeting the PD-1/PD-L1 pathway have been approved for use in over 20 tumor indications in the USA alone.[2]

Anti-PD-1/PD-L1 antibodies are finding increasing use in first-line therapy for metastatic cancer as well as at earlier stages of the disease. As these therapies achieve broader application, there is an increasing opportunity to look for therapeutic approaches that are more advantageous to patients. For instance, more convenient regimens and routes of administration are being developed for current ICIs, such as longer dosing intervals for intravenous delivery,[3] as well as formulations for intramuscular injection.

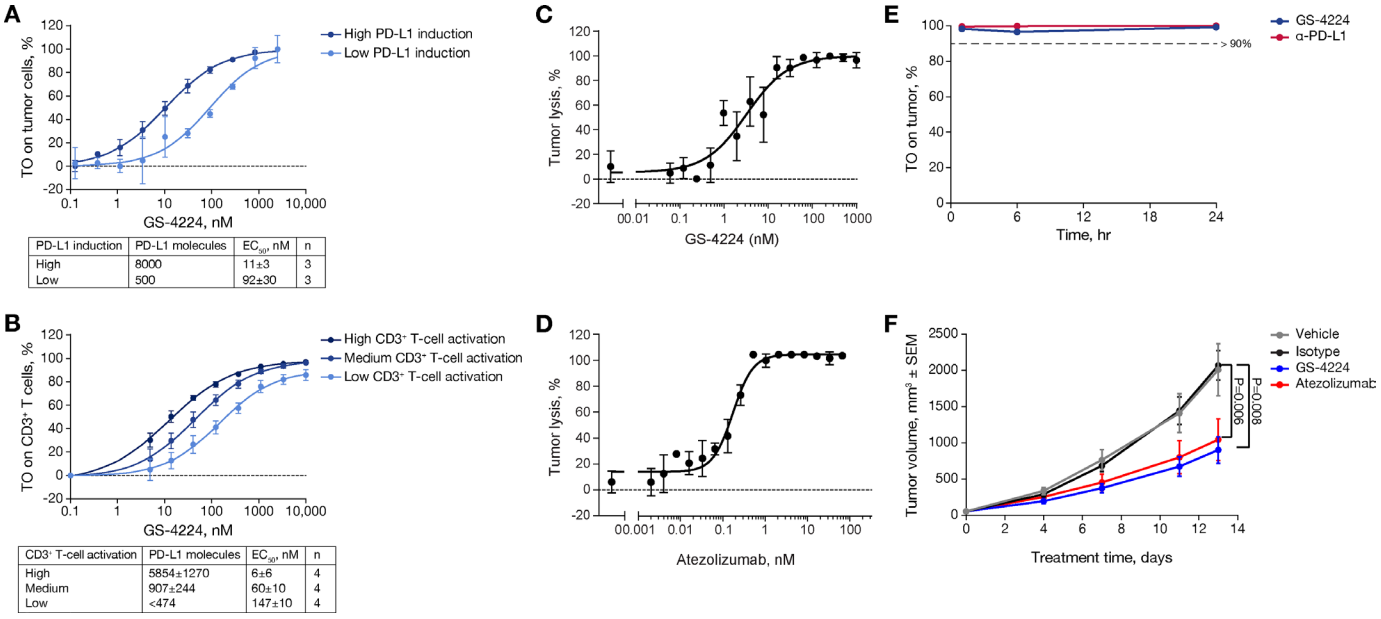

PD-L1 induction	PD-L1 molecules	EC_{50}, nM	n
High	8000	11±3	3
Low	500	92±30	3

CD3+ T-cell activation	PD-L1 molecules	EC_{50}, nM	n
High	5854±1270	6±6	4
Medium	907±244	60±10	4
Low	<474	147±10	4

Figure 1 Preclinical target occupancy and antitumor activity of GS-4224. Potentiation of GS-4224 with increasing PD-L1 expression on human tumor (A) and immune cells (B). (A) A549 lung cancer cells were treated with low (60 pg/mL) and high concentrations (20 ng/mL) of IFN-γ for 48 hours to induce low and high levels of cell surface PD-L1 expression with concomitant treatment of GS-4224 dose response to determine TO by flow cytometry in three independent experiments. (B) $CD3^+$ T cells were either left unstimulated or activated with α-CD3/α-CD28 and IL-2 to upregulate PD-L1 expression with concomitant treatment of GS-4224 dose response in four biological donors. At 48 hours, TO was measured by flow cytometry on non-activated (low PD-L1 levels), activated CD25 negative (medium PD-L1 levels), and activated CD25 positive (high PD-L1 levels) populations. GS-4224 (C) achieves a similar magnitude of tumor lysis in vitro as α-PD-L1 antibody, atezolizumab (D). Allogeneic $CD8^+$ T-cell tumor spheroid co-culture was established to assess T-cell-mediated lysis of MDA-MB-231-GFP human breast carcinoma cells. Tumor lysis was measured as a reduction in GFP signal and normalized to atezolizumab α-PD-L1 antibody control. GS-4224 induced T-cell-mediated lysis to a degree similar to atezolizumab. Data is plotted as a mean of three replicates per inhibitor concentration±SD. Results were reproduced in at least three independent donors and data from one representative experiment is shown. GS-4224 achieves >90% TO on HuMC38 tumor cells (E) and demonstrates comparable antitumor activity to α-PD-L1 antibody (F). (E) TO was determined by flow cytometry from tumors collected at 1, 6, and 24 hours post dosing on day 6 and measured as a reduction in PD-L1 MFI. (F) Mice implanted with MC38 tumor cells expressing human PD-L1 were treated with 25 mg/kg GS-4224 (blue), 10 mg/kg α-PD-L1 antibody atezolizumab (red), 10 mg/kg isotype control (black), or vehicle control (gray). Tumor volume was monitored throughout the duration of the study and TGI was determined post-dosing on day 13. At 25 mg/kg GS-4224 or 10 mg/kg α-PD-L1 antibody atezolizumab, TGI was similar (49–55%). EC_{50}, half maximal effective concentration; GFP, green fluorescent protein; IFN-γ, interferon gamma; MFI, median fluorescence intensity; PD-L1, programmed death ligand 1; TGI, tumor growth inhibition; TO, target occupancy.

Oral administration could offer increased convenience and control for patients.

An oral small molecule approach to PD-1/PD-L1 blockade could also help with the management of toxicities. Current guidelines recommend suspending ICI treatment when grade 2 or higher toxicities occur and to consider resuming therapy when they have resolved.[4] With more rapid clearance and reversal of target blockade after dose interruption, a small molecule inhibitor could provide an opportunity for more rapid management of adverse events (AEs) and, ultimately, returning patients to effective therapy.

GS-4224 (evixapodlin) is a PD-L1-binding symmetrical tetra aryl small molecule with a molecular weight of 691.6 g/mol. The structure was previously published.[5] Here, we describe preclinical data showing that GS-4224 is a potent, selective, and orally bioavailable inhibitor of PD-L1. We also present the results of a phase 1 clinical study evaluating the safety, tolerability, pharmacokinetics, biomarkers, and efficacy of GS-4224 in participants with advanced solid tumors.

METHODS

In vitro PD-L1 target occupancy assays

Green fluorescent protein (GFP)-expressing A549 lung adenocarcinoma cells were treated with a titration of GS-4224 in the presence of either 60 pg/mL interferon gamma (IFN-γ; low PD-L1 induction) or 20 ng/mL IFN-γ (high PD-L1 induction) for 48 hours. Free PD-L1 expression was detected by the addition of an atezolizumab analog with mouse IgG1 Fc followed by allophycocyanin-conjugated α-mouse IgG1 and analysis by flow cytometry.

For primary human $CD3^+$ T cells, peripheral blood mononuclear cells (PBMC) samples were either left unstimulated or stimulated for 48 hours with anti-CD3/CD28 and interleukin (IL)-2. After exposure to GS-4224, free PD-L1 expression on T cells was detected by staining

Table 1 Demographic and clinical characteristics

	Total population (N=18)
Sex at birth	
Male, n (%)	15 (83.3)
Female, n (%)	3 (16.7)
Biometrics	
Median age (range), years	63 (24–79)
Median weight (range), kg	82.1 (49.5–119.9)
Median body mass index (range), kg/m^2	26.8 (21–50)
Race	
White, n (%)	13 (72.2)
Asian, n (%)	2 (11.1)
Other, n (%)	3 (16.7)
Ethnicity	
Not Hispanic or Latino, n (%)	15 (83.3)
Hispanic or Latino, n (%)	3 (16.7)
Tumor histology	
RCC, n (%)	3 (16.7)
NSCLC, n (%)	2 (11.1)
Urothelial, n (%)	2 (11.1)
Mesothelioma, n (%)	2 (11.1)
Gastric/esophageal, n (%)	2 (11.1)
Other,* n (%)	7 (38.9)
ECOG PS	
0, n (%)	8 (44.4)
1, n (%)	10 (55.6)
Prior anticancer therapies	
≥2 prior therapies, n (%)	12 (66.7)
Surgery, n (%)	14 (77.8)
Chemotherapy, n (%)	13 (72.2)
Targeted agent therapy, n (%)	4 (22.2)
Radiation therapy, n (%)	9 (50.0)
Anti-PD-1/PD-L1, n (%)	2 (11.1)

*Endometrial cancer, uterine cancer, pancreatic cancer, TNBC, CRPC, anal carcinoma, and HCC.
CRPC, castration-resistant prostate cancer; ECOG PS, Eastern Cooperative Group performance status; HCC, hepatocellular carcinoma; NSCLC, non-small cell lung cancer; PD-1, programmed cell death protein 1; PD-L1, programmed cell death ligand 1; RCC, renal cell carcinoma; TNBC, triple-negative breast cancer.

with phycoerythrin (PE)-conjugated atezolizumab and analysis by flow cytometry. Target occupancy was normalized to saturated PD-L1 receptors.

For the in vitro peripheral human whole blood assay, blood samples were either left unstimulated or stimulated for 24 hours with IFN-γ. Following exposure to GS-4224, free PD-L1 expression on activated monocytes and resting, unstimulated T cells was detected by staining with PE-conjugated atezolizumab and analysis by flow cytometry. Target occupancy was normalized to saturated PD-L1 receptors.

Additional details for occupancy assays are listed in the online supplemental methods.

Tumor cell lysis assay

GFP-MDA-MB-231 cells cultured in 96-well plates were treated with titrations of anti-PD-L1 antibody (atezolizumab, Genentech) or GS-4224 were dispensed in triplicate. CD8$^+$ T cells were added at an effector-to-target ratio of 10:1. Tumor cells were imaged on an IncuCyte S3 (Essen BioScience, Ann Arbor, Michigan) and lysis was calculated from both phase contrast and green fluorescence image channels taken over 5–6 days, normalized to dimethyl sulfoxide (0% lysis) and to 10 µg/mL of anti-PD-L1 antibody (100% lysis). Additional details are listed in the online supplemental methods.

In vivo mouse tumor studies

Human PD-L1-overexpressing murine MC38 (HuMC38) colorectal tumor cells (Crown Bioscience) were implanted subcutaneously into the right flank of female C57BL/6 mice. Once tumors reached a mean volume of ~50 mm^3, mice were randomized (12 mice per group). Treatments were administered as an intraperitoneal injection and tumor growth was monitored by caliper measurement. To assess tumor target occupancy, tumors were harvested and dissociated, and single-cell suspensions were stained for cell lineage markers and free human PD-L1 (MIH1) and analyzed by flow cytometry. Target occupancy was calculated as the loss of PD-L1 fluorescence signal compared with control tumor cells. The procedures involving the care and use of animals in this study were reviewed and approved by the Institutional Animal Care and Use Committee of CrownBio (reference number AN-1702-008-278) prior to conduct. Additional study details are listed in the online supplemental methods.

Phase 1 study design

This was an open-label, multicenter, sequential dose-escalation study in patients with advanced solid tumors who had progressed after or who were intolerant of standard therapy or for whom no standard therapy exists. GS-4224 was administered once daily (QD), and dose escalation proceeded according to a standard 3+3 design. The starting dose was 400 mg, with subsequent doses of 700, 1,000, and 1,500 mg. Patients were treated until unacceptable toxicity, withdrawal of consent, disease progression, or death. The primary objectives were to characterize the safety and tolerability of GS-4224 and to determine the maximum tolerated dose and recommended phase 2 dose in participants with advanced solid tumors. The study was conducted at sites in New Zealand and the USA.

Biopsy substudy

At dose levels equal to or below the maximum tolerated dose, additional participants per dose level with biopsy accessible, PD-L1–positive tumor lesions (tumor

Table 2 Summary of treatment-emergent and treatment-related adverse events

TEAEs: overall summary					
n (%)	400 mg (n=5)	700 mg (n=3)	1,000 mg (n=7)	1,500 mg (n=3)	Total (N=18)
TEAE	5 (100)	3 (100)	7 (100)	3 (100)	18 (100)
TEAE with grade 3 or higher	1 (20)	2 (67)	2 (29)	1 (33)	6 (33)
TE serious AE	0	1 (33)	2 (29)	1 (33)	4 (22)
TEAE related to GS-4224	5 (100)	3 (100)	6 (86)	2 (67)	16 (89)
TEAE related to GS-4224 with grade 3 or higher	1 (20)	0	0	1 (33)	2 (11)
TEAE leading to discontinuation of GS-4224	0	0	1 (14)	1 (33)	2 (11)
TEAEs related to GS-4224 occurring in ≥10% of patients					
Any	5 (100)	3 (100)	6 (86)	2 (67)	16 (89)
Nausea	4 (80)	2 (67)	4 (57)	1 (33)	11 (61)
Diarrhea	2 (40)	1 (33)	4 (57)	1 (33)	9 (50)
Fatigue	2 (40)	1 (33)	1 (14)	1 (33)	5 (28)
Vomiting	1 (20)	1 (33)	1 (14)	2 (67)	5 (28)
Decreased appetite	0	0	1 (14)	1 (33)	2 (11)
Gastritis	0	0	1 (14)	1 (33)	2 (11)
Rash	2 (40)	0	0	0	2 (11)

TEAE, treatment-emergent adverse event.

proportion score ≥10% or combined positive score ≥10) were enrolled in a biopsy substudy to evaluate the GS-4224 tumor target occupancy of GS-4224 in post-treatment tumor biopsy samples. The biopsies collected were not adequate for evaluation.

Patient eligibility

Key inclusion criteria included histologically or cytologically confirmed advanced malignant solid tumor that was refractory to or intolerant of all available standard therapy, Eastern Cooperative Oncology Group performance status (ECOG PS)≤2, and adequate organ function. Patients who had received prior anti-PD-1/L1 antibodies were not excluded. Key exclusion criteria included the history of grade ≥3 AEs during prior treatment with an ICI, or a history of discontinuation of treatment with an ICI due to AEs and a history of autoimmune disease.

Safety assessments and dose escalation

Safety was evaluated by assessment of clinical laboratory tests, physical examination, 12-lead ECG, vital signs measurements, and the documentation of AEs. AEs were graded according to the National Cancer Institute Common Terminology Criteria for Adverse Events V.5.0 criteria.[6]

The safety and tolerability of each dose level was assessed by a safety review team after up to six participants enrolled in the dose level had been followed for at least 21 days after the first dose of GS-4224 or two dose-limiting toxicities were observed, whichever was earlier. The safety review team reviewed safety data and relevant clinical data and made the dose escalation, stay, or de-escalation decision based on the 3+3 design dose-escalation rules.

Pharmacokinetic assessments

Intensive pharmacokinetic samples for determination of GS-4224 plasma concentrations were collected on cycle 1 days 1 and 15 at the following time point: pre dose and 0.5, 1, 1.5, 2.5, 4, 6, and 24 hours post dose. GS-4224 plasma concentrations were analyzed using a fully validated high-performance liquid chromatography tandem mass spectroscopy bioanalytical method. The calibrated range was 10–10,000 ng/mL, and the inter-assay precision (% coefficient of variation (%CV)) and accuracy range (% relative error) were 3.17 to 4.95 and −3.20 to 3.87, respectively. All study samples were analyzed in the time frame supported by frozen stability storage data.

The following pharmacokinetic parameters for GS-4224 were calculated using non-compartmental analyses: time of maximum observed plasma concentration, maximum observed concentration, concentration at the end of the dosing interval and area under the concentration versus time curve over the dosing interval.

Response assessments

Response assessments were performed on cycle 3 day 1 and cycle 5 day 1 by CT with contrast, MRI, or positron emission tomography-CT scans. CT or MRI assessments were performed every 9 weeks after the cycle 5 assessment. Responses were evaluated according to Response Evaluation Criteria in Solid Tumors V.1.1 with modifications.[7]

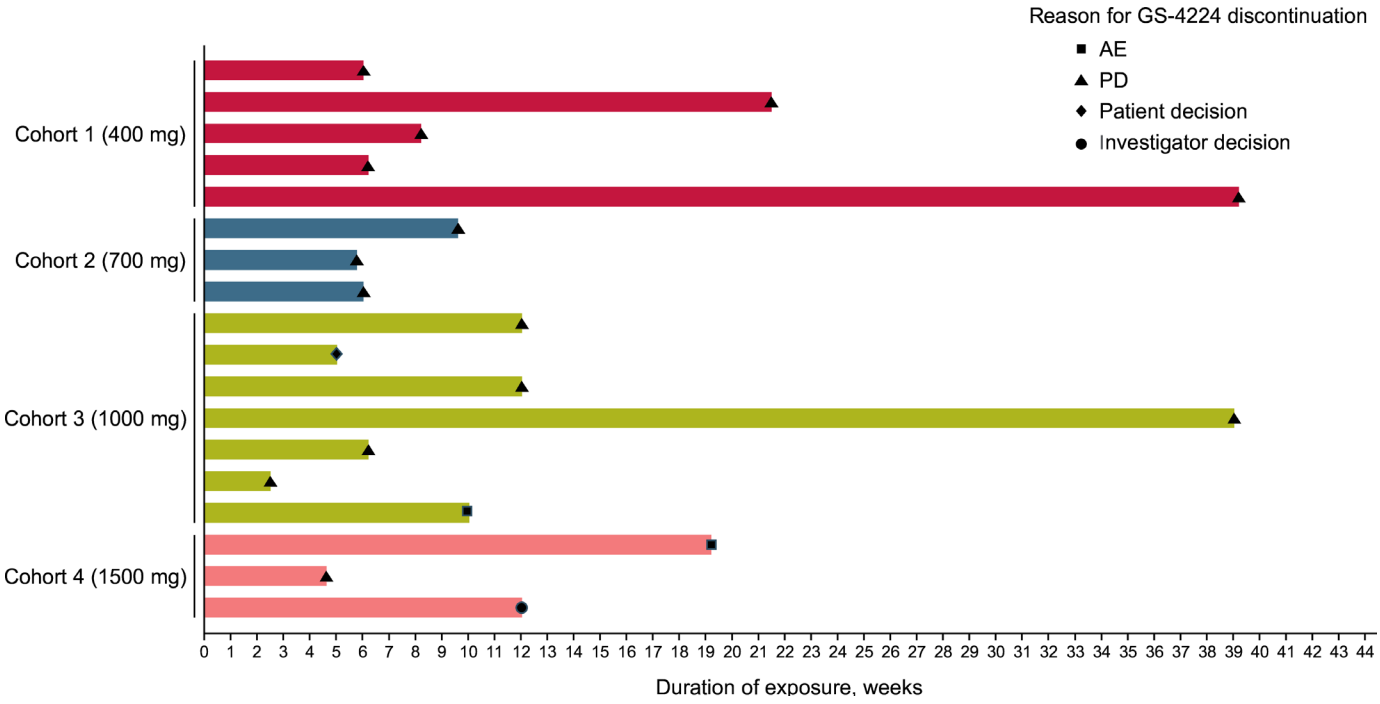

Figure 2 Treatment exposure. AE, adverse event; PD, progressive disease.

Tumor tissue analyses

PD-L1 status was collected based on local results. For patients with unknown status, PD-L1 immunohistochemistry was conducted retrospectively using the 22C3 clone. Samples were considered positive if they had a tumor proportion score of ≥1%, or a combined proportion score ≥1. DNA was extracted from remaining tissue and subjected to whole exome sequencing using SureSelect Human All Exon V.6 (Agilent; Santa Clara, California, USA) capture and Illumina sequencing (San Diego, California, USA).

Clinical PD-L1 target occupancy

PBMCs were isolated by Ficoll separation from heparinized patient blood samples and cryopreserved in 10% dimethyl sulfoxide CryoStor freezing media on the day of collection. Cryopreserved cells were transferred in batches to Primity Bio (Fremont, California, USA) for analysis. Cells were stained for CD45, CD3, CD4, CD8, CD45RA, viability dye, and free PD-L1 detection antibody. Prior to staining, a replicate sample was pretreated with an unlabeled PD-L1 blocking antibody as a positive control. The baseline amount of free PD-L1 was determined for each patient by subtracting the mean fluorescent intensity of free PD-L1 in the blocked control from that of the unblocked control. Occupancy was determined by dividing the amount of free PD-L1 detected on treatment by the baseline value and multiplying by 100.

Blood immunophenotyping

Cryopreserved PBMCs were analyzed for T-cell activation markers by flow cytometry at Primity Bio. Cells were stained for CD45, CD3, CD4, CD8, CCR7, CD45RA, PD-1, HLA-DR, Ki67, Foxp3, and a viability dye. The per cent activation marker positive was analyzed for each parent population, and the change and the per cent change from baseline were calculated.

T-cell receptor sequencing

Whole blood collected in ethylenediaminetetraacetic acid was frozen at −20°C until needed. Frozen blood samples were transferred to Adaptive Biotechnologies (Seattle, Washington, USA) for DNA extraction and analysis by ImmunoSEQ TCRB assay. Where available, DNA extracted from archival tumor tissue was also submitted for T-cell receptor (TCR) sequencing to identify clones shared between blood and tumor.

Serum cytokine analysis

Serum was collected from study participants, frozen on the day of collection, and stored at −20°C until analysis. Samples were analyzed in batches for 61 cytokines and chemokines using V-PLEX-validated assay panels at Meso Scale Diagnostics (Rockville, Maryland, USA). Nineteen analytes were excluded from the analysis because the majority of values were below the lower limit of quantitation. For the remaining analytes, hierarchical clustering was applied based on percentage change post-treatment.

Statistical analysis

Analysis of clinical outcomes and pharmacokinetic data was conducted according to prespecified criteria outlined in a statistical analysis plan. Biomarker data analyses were similarly prespecified in a biomarker analysis plan.

Patient and public involvement

Patients were not involved in the design, interpretation, or reporting of this study.

Table 3 GS-4224 plasma pharmacokinetic parameters (mean (%CV)) in participants with solid tumors

	400 mg (n=5)*		700 mg (n=3)		1,000 mg (n=6)†		1,500 mg (n=3)	
Parameter	Day 1	Day 15	Day 1	Day 15	Day 1	Day 15	Day 1	Day 15
C_{max} (ng/mL)	1090 (33)	1190 (51)	1470 (34)	1580 (16)	1920 (20)	2050 (34)	2120 (3)	2480 (11)
T_{max} (hour)‡	1.0 (0.75–2.5)	1.5 (1.0–4.0)	1.5 (1.0–2.5)	1.5 (1.0–1.5)	1.5 (1.0–1.7)	1.5 (1.0–2.5)	2.5 (2.5–6.0)	4.0 (1.5–6.0)
C_{trough} (ng/mL)	40.3 (24)	110 (32)	56.2 (32)	199 (29)	112 (39)	319 (28)	180 (12)	473 (24)
AUC_{tau} (ng·h/mL)	6,540 (27)	9,270 (29)	8,700 (43)	13,500 (23)	12,200 (23)	19,400 (27)	19,100 (3)	27,700 (28)

*The 400 mg dose level includes data from Cohort 1 (N=3) and Cohort 1 biopsy substudy (N=2).
†The 1000 mg dose level includes data from Cohort 3; data were not available for the participants in Cohort 3 biopsy substudy.
‡Median (first quartile (Q1), third quartile (Q3)) are presented for T_{max}.
AUC_{tau}, area under the concentration versus time curve over the dosing interval; C_{max}, maximum observed concentration; C_{trough}, concentration at the end of the dosing interval; %CV, % coefficient of variation; T_{max}, time to maximum observed plasma concentration.

RESULTS

GS-4224 leads to PD-L1 dimerization

To evaluate the impact of GS-4224 on cell surface PD-L1, a split luciferase system called NanoBiT was established. When the two subunits are expressed and brought into close proximity to form a functional enzyme, a luminescent signal can be detected with a cell-permeable substrate (online supplemental figure 1A). GS-4224 dose-dependent enhancement of luminescent signal was observed for PD-L1 expressing cells but not for PD-L2 (online supplemental figure 1B), indicating that GS-4224 selectively dimerizes PD-L1. Structural studies of the GS-4224 co-crystalized with the PD-L1 extracellular domain showed that GS-4224 binds two PD-L1 molecules in a ligand-induced, homodimeric fashion (data not shown).

GS-4224 potency is PD-L1 concentration dependent

Simulations of the kinetics of GS-4224/PD-L1 ternary complex formation predicted that cell surface density would influence GS-4224 binding potency. To test this hypothesis, PD-L1 target occupancy by GS-4224 was evaluated in human A549 adenocarcinoma cells with or without upregulation of PD-L1 via IFN-γ. The average half maximal effective concentration (EC_{50}) for target occupancy was 11±3 nM for high levels (8,000 molecules/cell) of PD-L1 and 92±30 nM for low levels (500 molecules/cell) of PD-L1 (figure 1A). A similar study was performed on ex vivo human $CD3^+$ T cells expressing low levels of PD-L1 (<474 PD-L1 molecules/cell). To upregulate PD-L1 expression, T cells were activated with anti-CD3/CD28 antibodies and recombinant IL-2. By 48 hours, activated $CD3^+$ T cells were separated into low activation (CD25 negative, <474 PD-L1 molecules/cell), medium activation (CD25 low, 907 PD-L1 molecules/cell), and high activation (CD25 high, 5,854 PD-L1 molecules/cell) populations. The average target occupancy (TO) EC_{50} potency shifted from 147±10 (PD-L1 low) to 60±10 (PD-L1 medium) to 6±6 nM (PD-L1 high), corresponding to the enhanced number of PD-L1 molecules (figure 1B). Overall, GS-4224 binding to PD-L1 on primary human $CD3^+$ T cells was >20-fold more potent on cells that were PD-L1 high versus low. These results suggest that GS-4224 will readily occupy PD-L1 on cells expressing high PD-L1 levels, but that higher concentrations of GS-4224 will be required to drive target occupancy on cells with lower levels of PD-L1.

GS-4224 has preclinical antitumor activity

To assess the antitumor activity of GS-4224 in vitro, a three-dimensional tumor spheroid co-culture assay was established in which human $CD8^+$ T cells from HLA-$A2^+$ donors were cultured with GFP-expressing HLA-$A2^+$ MDA-MB-231 breast carcinoma cells. GS-4224 enhanced tumor cell killing with an average potency of 12±15 nM (figure 1C). Importantly, the maximum magnitude of GS-4224-mediated killing was comparable to the anti-PD-L1 antibody, atezolizumab (figure 1D). Supernatants

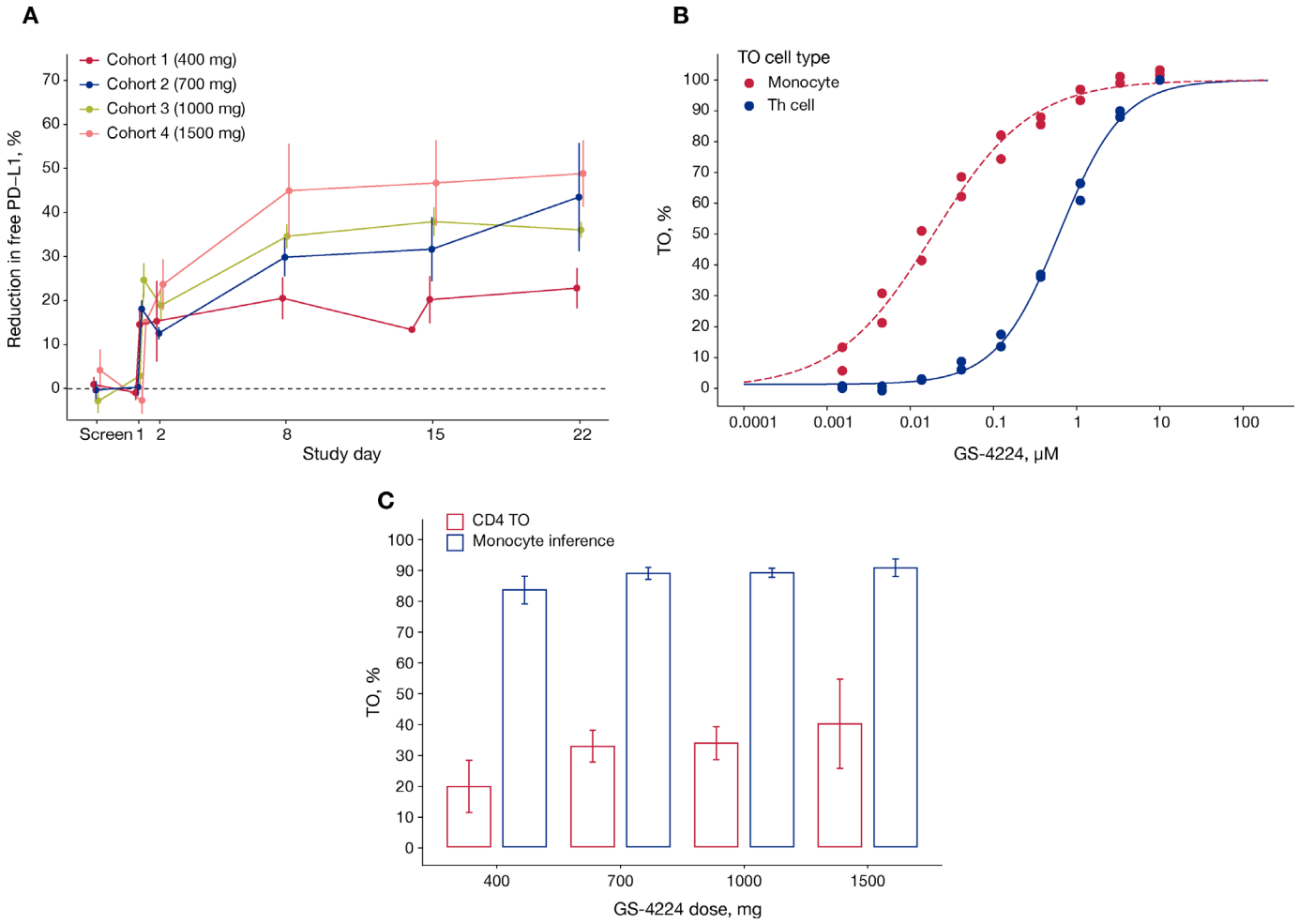

Figure 3 PD-L1 target occupancy. (A) Per cent reduction in free PD-L1. (B) Ex vivo dose-response curve in monocytes and Th cells. (C) Observed median target occupancy on CD4 T cells (Th cells) and inferred median target occupancy on IFN-γ-activated monocytes on cycle 1 day 8. IFN-γ, interferon gamma; PD-L1, programmed death ligand 1; TO, target occupancy.

collected at the end of the co-culture also demonstrated similar elevation of IFN-γ and granzyme B for both GS-4224 and atezolizumab, confirming the tumor lysis was elicited by T cells (data not shown).

In vivo activity of GS-4224 was assessed using MC38 tumor cells expressing human PD-L1 since GS-4224 does not bind murine PD-L1. Biochemical experiments showed that GS-4224 blocks the interaction between mouse PD-1 and human PD-L1 (data not shown). At 25 mg/kg GS-4224 or 10 mg/kg anti-PD-L1 antibody atezolizumab, >90% TO on the tumor cells was observed for at least 24 hours (figure 1E). This binding was associated with similar tumor growth inhibition from 49% to 55% for both GS-4224 and the anti-PD-L1 antibody atezolizumab (figure 1F). Moreover, there was no treatment-related effect on body weight, indicating GS-4224 was well tolerated for the duration of the study.

Phase 1 study patient characteristics

The safety, tolerability and pharmacokinetics of GS-4224 were evaluated in an open-label dose-escalation study. Between August 2019 and March 2021, 18 patients with advanced solid tumors were enrolled and received the study drug at two sites in the USA and two sites in New Zealand. Cohorts 1–4 were dosed at 400 (n=3), 700 (n=3), 1,000 (n=6), and 1,500 mg (n=3), respectively. Additionally, three patients were enrolled in a biopsy substudy at 400 (n=2) and 1,000 mg (n=1) dose levels. The study was discontinued for business reasons and no further dose escalation or dose expansion was conducted. Table 1 summarizes patient demographics and baseline characteristics. The median age of the participants was 63 years (range, 24–79 years); 15 participants (83.3%) were born men. At baseline, 8 participants had an ECOG PS of 0 (44.4%) and 10 participants had an ECOG PS of 1 (55.6%). Patients were heavily pretreated, with 66.7% of patients having had ≥2 and ≤8 prior anticancer regimens.

Unless participating in the biopsy substudy, patients were not required to have PD-L1-positive tumors to be enrolled. For patients with unknown local PD-L1 status and for whom tumor tissue was available, PD-L1 expression was determined retrospectively. Individual patient diagnoses, prior checkpoint inhibitor treatment, PD-L1 status, and tumor mutation burden (TMB) are listed in online supplemental table 1. Of the 13 participants

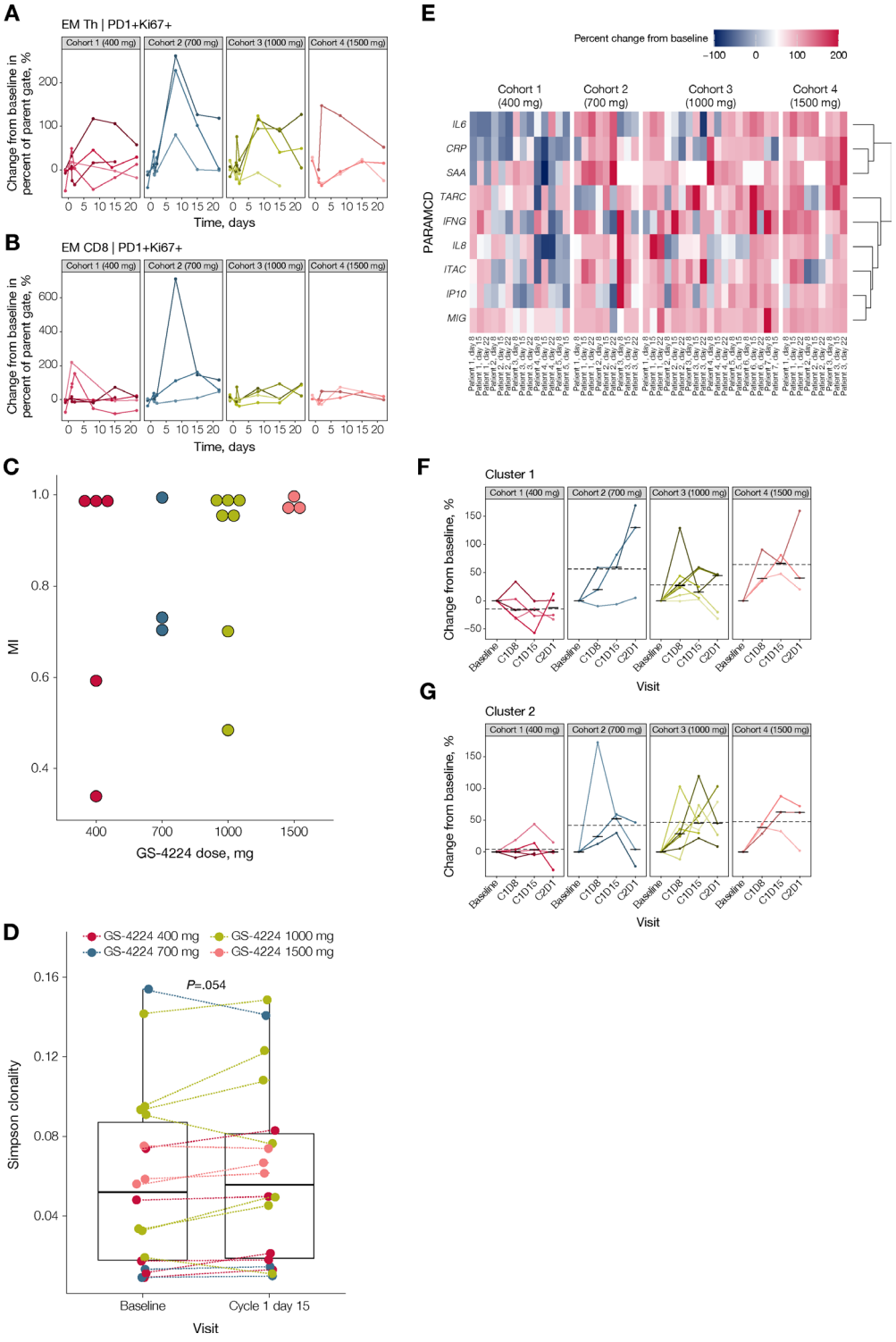

Figure 4 Immunological and pharmacodynamic responses. (A) Per cent change from baseline in Th cells. Colored lines represent data from participants in each dose cohort. (B) Per cent change from baseline in CD8 T cells. Colored lines represent data from participants in each dose cohort. (C) Morisita Index across GS-4224 dose cohorts. (D) Simpson clonality at baseline and cycle 1 day 15. (E) Per cent change from baseline in the expression of select cytokines and chemokines. (F) Per cent change from baseline in cluster mean in cluster 1 cytokines (CRP, IL-6, SAA). Colored lines represent data from participants in each dose cohort. Dashed lines represent the mean value from C1D8 to C2D1. Solid black lines represent the median. (G) Per cent change from baseline in cluster mean for cluster 2 cytokines (GROA, IFN-γ, IL-17b, IL-8, IP-10, ITAC, MIP3A, and TARC). Colored lines represent data from participants in each dose cohort. Dashed lines represent the mean (excluding baseline). Solid black lines represent the median. C, cycle; CRP, C reactive protein; d, day; EM, effector memory; GROA, C-X-C motif chemokine ligand 1; IFN-γ, interferon gamma; IL, interleukin; IP-10, C-X-C motif chemokine ligand 10; ITAC, C-X-C motif chemokine ligand 11; MI, Morisita Index; MIP3A, C-C motif chemokine ligand 20; PD-1, programmed death 1; SAA, serum amyloid A cluster; TARC, C-C motif chemokine ligand 17.

with available PD-L1 results, 9 were PD-L1 positive. Four participants had a PD-L1 tumor proportion score ≥50%. For participants with available whole exome sequencing data, we estimated TMB, and six of seven of these were TMB low (<16 mutations/Mb).

Clinical safety and efficacy

There were no dose-limiting toxicities up to and including the highest dose of 1,500 mg. Four participants (22.2%) experienced serious AEs, and two participants (11.1%) discontinued treatment due to AEs. Treatment-emergent AEs (TEAEs) assessed by the investigator to be related to GS-4224 were reported in 16 of 18 participants (88.9%). The most common TEAEs related to GS-4224 by cohort and preferred term are presented in table 2. Six patients (33.3%) experienced grade ≥3 TEAEs. These included cancer pain, deep vein thrombosis, gastrointestinal hemorrhage, lower respiratory tract infection, norovirus infection, pulmonary embolism, fever, rash, rectal perforation, sepsis, and small intestinal obstruction. Gastrointestinal hemorrhage and rash were deemed related to GS-4224 by the investigator. No individual grade ≥3 TEAE occurred in >1 participant.

No objective responses were observed. Seven patients had a best overall response of stable disease. Duration of exposure and per cent change in target lesion from baseline are shown in figure 2 and online supplemental figure 2, respectively.

Pharmacokinetics

Pharmacokinetic parameters of GS-4224 on days 1 and 15 of cycle 1 in participants with solid tumors are presented in table 3.

PD-L1 target occupancy

Using a GS-4224-competitive PD-L1 detection antibody that does not bind in the presence of GS-4224-mediated dimerization, we were able to estimate the fraction of cell surface target bound by GS-4224 in the blood of treated patients. Target occupancy, as inferred by a reduction in free, unbound surface PD-L1 on blood T cells, was observed at all dose levels after a single dose and reached a plateau within 1 week of dosing, reaching a median of 40.2% target occupancy at the trough at 1,500 mg QD (figure 3A). The mean steady-state trough exposure of 473 ng/mL (684 nM) at this dose level was predicted to be associated with 53% target occupancy on Th cells in a preclinical in vitro whole blood dose-response curve (figure 3B), in reasonable agreement with the clinically observed target occupancy.

Since prior experiments demonstrated that GS-4224 potency is dependent on PD-L1 density, a whole blood in vitro model was established to extrapolate observed target occupancy on resting (unstimulated) blood T cells (PD-L1 low, 109 molecules/cell) to predicted target occupancy on IFN-γ-activated monocytes (PD-L1 high, 21,583 molecules/cell). In human whole blood, consistent with prior experiments, GS-4224 binding to PD-L1 was more potent on IFN-γ-activated monocytes than on resting T cells (figure 3B). Using these data to extrapolate from the observed clinical target occupancy measured on T cells, the reduction of free PD-L1 on activated monocytes was predicted to be ≈90% at doses of 700 mg or higher (figure 3C).

Immunological pharmacodynamic responses

Treatment with a PD-1 antibody leads to a proliferative burst of peripheral T cells in a subset of patients who are more likely to have an objective response.[8] To measure the effect of GS-4224 on T-cell activation, the change in activation marker Ki67 was analyzed on peripheral blood T cells. PD-1-positive cells were expected to respond to PD-1/PD-L1 blockade,[9] and we found that PD-1 expression was highest on central memory (CD45RA– CCR7+) and effector memory (CD45RA– CCR7–) subsets of both the CD4 and CD8 lineages, along with CD4+Foxp3+ T cells, by flow cytometry (data not shown). After treatment with GS-4224, some patients showed an increase in Ki67 among the PD-1-positive T-cell subsets (figure 4A,B), particularly effector memory CD4 T cells, consistent with functional blockade of PD-L1.

TCR beta chain sequencing was performed to determine if the change in activation markers was associated with clonal expansion. Based on a reduction in Morisita Index, changes in the blood TCR repertoire were observed in six participants (figure 4C) at different dose levels. The Simpson clonality, which would be expected to increase with clonal expansion, was numerically but modestly increased 2 weeks post-treatment but was not statistically significant (figure 4D). For tumor-associated clones, that is, TCR clones that were found both in tumor and blood at baseline, there was no change in on-treatment versus pretreatment blood frequency (online supplemental figure 4).

To further characterize the immune response induced by GS-4224, we measured serum cytokines/chemokines by multiplex immunoassay. Hierarchical clustering of cytokine/chemokine changes post-treatment revealed two clusters of co-regulated proteins: cluster 1 represented by acute phase proteins IL-6, C reactive protein, and serum amyloid A; and cluster 2 containing IFN-γ and the IFN-related chemokines CXCL9/monokine induced by IFN-γ, CXCL10/IFN-γ-inducible protein-10, and CXCL11/IFN-inducible T-cell alpha chemoattractant (online supplemental figure 3). The heatmap of proteins in these two clusters is shown in figure 4E. Average protein levels in clusters 1 and 2 increased by approximately 50% and 30%, respectively, after GS-4224 treatment at the 700 mg dose level and above (figure 4F, G). These patterns were consistent with what has been reported for atezolizumab.[10]

DISCUSSION

GS-4224 is an orally bioavailable, selective inhibitor of PD-L1 that binds specifically to PD-L1, induces dimerization, and thereby inhibits interaction with PD-1 leading

to immune cell activation in vitro and antitumor efficacy in vivo. This unique ligand dimerization mode of action causes the potency of GS-4224 to be proportional to the density of PD-L1 molecules on the target cells. Using a primary T-cell model system, we showed that potency was more than 80-fold greater on highly activated cells (~5,800 PD-L1 molecules/cell) versus resting T cells (<474 molecules/cell). Notably, the commonly used PD-L1 immunohistochemistry (IHC) 22C3 pharmDx has a lower limit of detection of 200,000–400,000 molecules/cell,[11] suggesting that PD-L1+tumor cells and tumor-associated immune cells that can be detected by IHC express many more molecules of PD-L1 per cell than the activated T-cell model. In our whole blood model, IFN-γ activated monocytes expressed 21,583 PD-L1 molecules/cell whereas resting Th cells expressed 109 PD-L1 molecules/cell. These data suggest that GS-4224 is more efficient at blocking the target on PD-L1 high tumor cells or antigen-presenting cells than on resting immune cells with lower PD-L1 levels.

During dose escalation, an approximately dose-proportional increase in GS-4224 plasma exposure (AUC) was observed in the 400–1,500 mg QD dose range, with moderate pharmacokinetic variability. GS-4224 peak plasma concentrations were reached within 1.0–4.0 hours after GS-4224 dosing, on average. The increase in GS-4224 exposure was approximately dose-proportional in the evaluated dose range. GS-4224 AUC was 45–60% higher at steady-state compared with day 1, consistent with an effective half-life of approximately 14–17 hours.[12] Overall, the pharmacokinetic characteristics of GS-4224 supported QD dosing.

We observed a dose-dependent reduction in free PD-L1 on peripheral blood T cells, with a median reduction of ≈40% at 1,500 mg QD, at trough. PD-L1 target occupancy was measured on peripheral blood T cells because these cells are readily accessible and, unlike monocytes, maintain a stable level of PD-L1 expression through PBMC processing and cryopreservation. This stability allowed for batched analysis of longitudinally collected samples. However, PD-L1 levels on T cells are relatively low compared with the therapeutically relevant target cells in the tumor, and therefore extrapolation to predicted target occupancy on PD-L1 high cells was needed. To do this, we developed a whole blood in vitro model to translate observed target occupancy on resting blood T cells to predicted target occupancy on activated monocytes. Based on this model, the reduction of free PD-L1 on activated monocytes was predicted to be ≈90% at doses of ≥700 mg, which was expected to be sufficient for antitumor activity as shown in the preclinical mouse efficacy model.

Effective blockade of PD-L1 on antigen-presenting cells would be expected to release the inhibition of PD-1-positive T cells and lead to activation, observable as an increase in activated T cells, cytokine responses, and/or TCR clonal expansion. Some participants showed upregulation of the activation marker Ki67 on PD-1-positive T-cell subsets, particularly effector memory CD4 T cells. Ki67 responses were not seen in all patients, as is the case with antibody therapeutics and were spread across dose levels. Multiplex cytokine analysis showed a systemic increase in serum cytokines, particularly cytokine clusters related to IL-6 and IFN-γ, at ≥700 mg. In total, the weight of evidence suggests that GS-4224 has the intended effect of blocking PD-1/PD-L1 interactions in a biologically relevant way, leading to the activation of an immune response. Given the small patient numbers, different patient populations, and differences in assay methods, it is unclear if the magnitude and prevalence of these T-cell responses were equivalent to those reported for anti-PD-1 and/or anti-PD-L1 antibodies.

Treatment with GS-4224 was associated with an acceptable safety profile for the advanced solid tumor patient population. There were no dose-limiting toxicities among the 18 participants who received GS-4224 up to 1,500 mg QD. Despite achieving the expected progressive disease effects, no objective responses were observed among the 18 patients treated during this dose-escalation study. Further development of GS-4224 was discontinued by the study sponsor in favor of a PD-1/PD-L1 pathway antagonist that was more advanced in clinical testing. Since patients were not selected for checkpoint-responsive tumor types or biomarker profiles, a question remains as to whether objective responses should have been expected. Given the multiple lines of prior therapy and the overall small number of participants in this study, evaluation of GS-4224 in an adequate cohort of PD-1/PD-L1 therapeutic-naive, PD-L1-positive checkpoint responsive tumor types is needed to clearly assess its clinical activity.

Other small molecule PD-L1 inhibitors have been reported, including macrocyclic peptides, peptide mimetics, and other small molecules.[13] Like GS-4224, INCB086550 is a clinical-stage inhibitor that operates via a dimerization mechanism and shows increased potency with higher PD-L1 expression.[14] In an ex vivo IFN-γ stimulated whole blood assay, treatment with INCB086550 at 200 mg two times per day achieved an 85% reduction in free PD-L1, comparable to the reduction we estimate on IFN-γ stimulated monocytes at 400 mg GS-4224 QD. The authors report elevations in IFN-related cytokines in a subset of treated patients, consistent with our data. Inhibition of PD-L1 using orally administered small molecules is a promising and expanding pharmacological approach to immuno-oncology therapy.

Acknowledgements The authors would like to acknowledge the patients who participated in this study and their families. In addition, we acknowledge Raghad Abdul-Karim, Edward Gane, and Jorge Chaves for enrolling participants on the clinical trial, along with study site staff.

Contributors JMO designed, analyzed, and interpreted clinical biomarker experiments and led generation of the manuscript. AAO designed, analyzed, and interpreted the clinical study including the pharmacokinetics data. K-WL performed bioinformatic and statistical analysis of biomarker data. AYW designed, analyzed, and interpreted preclinical experiments and wrote the preclinical sections. JN developed and performed biomarker assays. OKY supervised clinical biomarker data analysis. JL led the bioanalytical method development and validation and oversaw generation of GS-4224 concentration data in the clinical

study. LL led the research team and contributed to data interpretation. PRD contributed to biomarker sample collection and processing. DT was the medical monitor for the clinical study. EA, NW, and SD enrolled patients on the study. All authors contributed to drafting, reviewing, and/or editing the manuscript and approved it for publication. JMO is responsible for the overall content and serves as guarantor.

Funding This study was funded by Gilead Sciences.

Competing interests JMO, AAO, K-WL, AYW, JN, OKY, JL, LL, and DT are employees and stockholders of Gilead Sciences. PRD, EA, NW, and SD received research funding from Gilead Sciences for the purposes of this study.

Patient consent for publication Not applicable.

Ethics approval The study was approved by the Western Institutional Review Board, Puyallup, Washington, USA (ref# 20191544); IntegReview Ethical Review Board, Austin, Texas, USA (ref# NXSAT19.08); Health and Disability Ethics Committees, Wellington, New Zealand (ref# 19/NTA/102/AM14); and Institutional Animal Care and Use Committee of CrownBio (ref # AN-1702-008-278). Participants gave informed consent to participate in the study before taking part.

Provenance and peer review Not commissioned; externally peer reviewed.

Data availability statement Gilead Sciences shares anonymized individual patient data upon request or as required by law or regulation with qualified external researchers based on submitted curriculum vitae and reflecting no conflict of interest. The requested proposal must also include a statistician. Approval of such requests is at Gilead Science's discretion and is dependent on the nature of the request, the merit of the research proposed, the availability of the data, and the intended use of the data. Data requests should be sent to datarequest@gilead.com.

ORCID iDs
Jared M Odegard http://orcid.org/0009-0005-6516-0026
Ahmed A Othman http://orcid.org/0000-0002-4937-2775

REFERENCES

1 Keir ME, Butte MJ, Freeman GJ, *et al*. PD-1 and its ligands in tolerance and immunity. *Annu Rev Immunol* 2008;26:677–704.
2 Vaddepally RK, Kharel P, Pandey R, *et al*. Review of indications of FDA-approved immune checkpoint inhibitors per NCCN guidelines with the level of evidence. *Cancers (Basel)* 2020;12:738.
3 Lala M, Li TR, de Alwis DP, *et al*. A six-weekly dosing schedule for pembrolizumab in patients with cancer based on evaluation using modelling and simulation. *Eur J Cancer* 2020;131:68–75.
4 Schneider BJ, Naidoo J, Santomasso BD, *et al*. Management of immune-related adverse events in patients treated with immune checkpoint inhibitor therapy: ASCO guideline update. *JCO* 2021;39:4073–126.
5 Chai I, Kornyeyev D, Hsieh E, *et al*. Effects of small molecule-induced dimerization on the programmed death ligand 1 protein life cycle. *Sci Rep* 2022;12:21286.
6 National Cancer Institute. Division of cancer treatment & diagnosis. common terminology criteria for adverse events (CTCAE). Available: https://ctep.cancer.gov/protocoldevelopment/electronic_applications/ctc.htm [Accessed 5 Feb 2024].
7 Eisenhauer EA, Therasse P, Bogaerts J, *et al*. New response evaluation criteria in solid tumours: revised RECIST guideline (version 1.1). *Eur J Cancer* 2009;45:228–47.
8 Kamphorst AO, Pillai RN, Yang S, *et al*. Proliferation of PD-1+ CD8 T cells in peripheral blood after PD-1-targeted therapy in lung cancer patients. *Proc Natl Acad Sci U S A* 2017;114:4993–8.
9 Herbst RS, Soria J-C, Kowanetz M, *et al*. Predictive correlates of response to the anti-PD-L1 antibody MPDL3280A in cancer patients. *Nature* 2014;515:563–7.
10 Powles T, Eder JP, Fine GD, *et al*. MPDL3280A (anti-PD-L1) treatment leads to clinical activity in metastatic bladder cancer. *Nature* 2014;515:558–62.
11 Sompuram SR, Torlakovic EE, 't Hart NA, *et al*. Quantitative comparison of PD-L1 IHC assays against NIST standard reference material 1934. *Modern Pathology* 2022;35:326–32.
12 Boxenbaum H, Battle M. Effective half-life in clinical pharmacology. *J Clin Pharmacol* 1995;35:763–6.
13 Ganesan A, Ahmed M, Okoye I, *et al*. Comprehensive in vitro characterization of PD-L1 small molecule inhibitors. *Sci Rep* 2019;9:12392.
14 Koblish HK, Wu L, Wang L-CS, *et al*. Characterization of INCB086550: a potent and novel small-molecule PD-L1 inhibitor. *Cancer Discov* 2022;12:1482–99.